applied sciences

MDPI

Article

Sub-Rectangular Tunnel Behavior under Seismic Loading

Van Vi Pham [1], Ngoc Anh Do [1,2] and Daniel Dias [3,4,*]

[1] Department of Underground and Mining Construction, Faculty of Civil Engineering, Hanoi University of Mining and Geology, Hanoi 100000, Vietnam; phamvanvi0410@gmail.com (V.V.P.); nado1977bb@gmail.com (N.A.D.)
[2] Sustainable Development in Underground Engineering Research Team, Hanoi University of Mining and Geology, Hanoi 100000, Vietnam
[3] Laboratory 3SR, Grenoble Alpes University, 38000 Grenoble, France
[4] Geotechnical Expert, Antea Group, 92160 Antony, France
* Correspondence: daniel.dias@3sr-grenoble.fr

Abstract: Circular and rectangular tunnel shapes are usually chosen when excavating at shallow depths in urban areas. However, special-shaped tunnels such as sub-rectangular tunnels have recently been used to overcome some drawbacks of circular and rectangular tunnels in terms of low space utilization efficiency and stress concentration, respectively. In the literature, experimental studies as well as analytical and numerical models have been developed for the seismic analysis and vulnerability assessment of circular and rectangular tunnels since the early 1990s. However, knowledge gaps regarding the behavior of sub-rectangular tunnels under seismic loading remain and still need to be bridged. The present paper focuses on introducing a numerical analysis of sub-rectangular tunnels under seismic loading. The numerical model of sub-rectangular tunnels is developed based on the numerical analyses of circular tunnels validated by comparing well-known, analytical solutions. This paper aims to highlight the differences between the behavior of sub-rectangular tunnels compared with circular tunnels when subjected to seismic loadings. Special attention is paid to the soil–lining interface conditions. The influence of parameters, such as soil deformations, maximum horizontal acceleration, and lining thickness, on sub-rectangular tunnel behavior under seismic loading is also investigated. The results indicate a significant behavior difference between sub-rectangular and circular tunnels. The absolute extreme incremental bending moments for a circular tunnel (no-slip condition) are smaller than that for the corresponding full-slip condition. The absolute extreme incremental bending moments of sub-rectangular tunnels (no-slip condition) are, however, greater than the corresponding full-slip conditions.

Keywords: sub-rectangular tunnel; seismic load; tunnel lining; numerical analysis

Citation: Pham, V.V.; Do, N.A.; Dias, D. Sub-Rectangular Tunnel Behavior under Seismic Loading. *Appl. Sci.* **2021**, *11*, 9909. https://doi.org/10.3390/app11219909

Academic Editor: Andrea Paglietti

Received: 3 October 2021
Accepted: 19 October 2021
Published: 23 October 2021

Highlights

- Two-dimensional numerical analyses of circular and sub-rectangular tunnels under seismic loading.
- The behavior of a sub-rectangular tunnel under seismic loading is significantly different from that of a circular tunnel.
- Effects of horizontal acceleration, the soil Young's modulus, lining thickness, and soil–lining interface are presented.

1. Introduction

Circular- and rectangular-shaped tunnels are frequent choices when such structures are excavated at shallow depths [1–4], particularly in urban areas. The main disadvantage of a circular tunnel is its small space utilization ratio. Compared to circular tunnels, rectangular tunnels provide a major part of their cross-section area for utilization purposes. However, their shape can induce stress concentrations at the tunnel corners, which can

be followed by failures of the supporting structure. Special-shaped tunnels based on a combination of circular and rectangular shapes can be a good solution, as they have a higher space utilization efficiency than that of circular tunnels. They also help to eliminate stress concentrations at the corners [5] and can have a greater bearing capacity. A special-shaped tunnel, namely, the sub-rectangular tunnel, was therefore recently used to improve the efficiency of underground space use [6–8]. This tunnel shape can be used in both excavation methods, i.e., cut-and-cover excavation and mechanized shield tunneling [8].

The behavior of circular and rectangular tunnels under seismic loading has been thoroughly studied in the literature [9–18]. Recently, Tsinidis et al. [19] introduced a state-of-the-art study on the seismic behavior of tunnels. Accordingly, experimental studies, analytical models, simplified methods, and numerical schemes for the seismic analysis and vulnerability assessment of circular and rectangular tunnels were extensively developed. However, knowledge gaps regarding the behavior of sub-rectangular tunnels under seismic loading and even under static loading still remain and need to be bridged. There are only a few studies investigating the structural behavior of sub-rectangular tunnels under static loading through full-scale or reduced-scale tests [6,7,20,21] and numerical analyses [22,23].

The construction of a tunnel is a three-dimensional (3D) process. However, due to the calculation time and modeling complexity, two-dimensional (2D) simulations are often adopted [16,24,25]. In the present study, a 2D finite-difference numerical model of a sub-rectangular tunnel under seismic loading is proposed. It is developed based on the modeling of a circular tunnel, which is validated by comparing the results obtained using well-known analytical solutions [9,12,16]. Parameters such as soil deformations, maximum horizontal acceleration, and lining thickness on the tunnel behavior under seismic loadings were carefully examined, and their influence was evaluated. In the study, particular attention was drawn to analyzing the soil–lining interface. Different behaviors of sub-rectangular- and circular-shaped tunnels under seismic loadings were compared based on numerical modeling.

2. Numerical Models

2.1. Reference Sub-Rectangular Tunnel Case Study—Shanghai Metro Tunnel

Parameters of a sub-rectangular express tunnel in Shanghai, China, are used as the reference case in this study [22]. The sub-rectangular tunnel dimensions are 9.7 m in width and 7.2 m in height (Figure 1). The tunnel is supported by a segmental concrete lining of 0.5 m. For simplification purposes, a continuous lining was adopted without considering the effect of joints. Based on this reference sub-rectangular tunnel, a circular tunnel with an external diameter of 4.89 m, which has an equivalent utilization space area, is considered for comparison purposes (Figure 2).

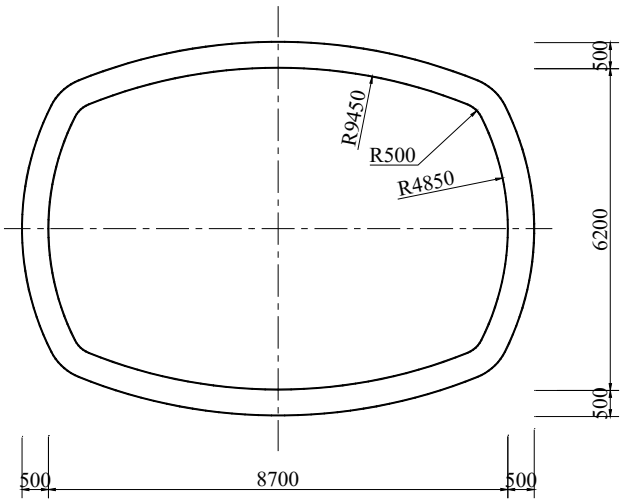

Figure 1. Sub-rectangular express tunnel in Shanghai [22], distances in millimeters.

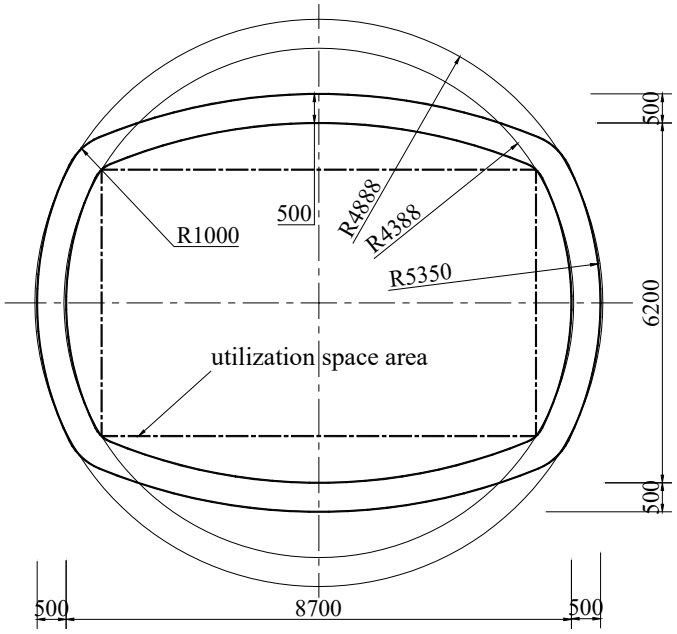

Figure 2. Circular tunnel with the same utilization space area, distances in millimeters.

2.2. Numerical Model for the Circular Tunnel

Firstly, a numerical model for circular tunnels was developed using a finite difference program (FLAC^{3D}) [24]. The purpose was to investigate the behavior of circular tunnel linings under quasi-static loading and make a comparison with those obtained by an analytical solution.

A 2D plane strain model was created (Figure 3). The soil mass is discretized into hexahedral zones. The tunnel lining is modeled using embedded liner elements, which are attached to the zone faces along the tunnel boundary with interfaces. Two interface conditions were considered: no slip between the soil and lining and full slip. The liner–zone interface stiffness (normal stiffness k_n and tangential stiffness k_s) is determined based on a given rule of thumb [24]. k_n and k_s are set equal to 100 times the equivalent stiffness of the stiffest neighboring zone [24] for the no-slip condition case. When considering the full-slip condition, k_s is assigned to be equal to zero.

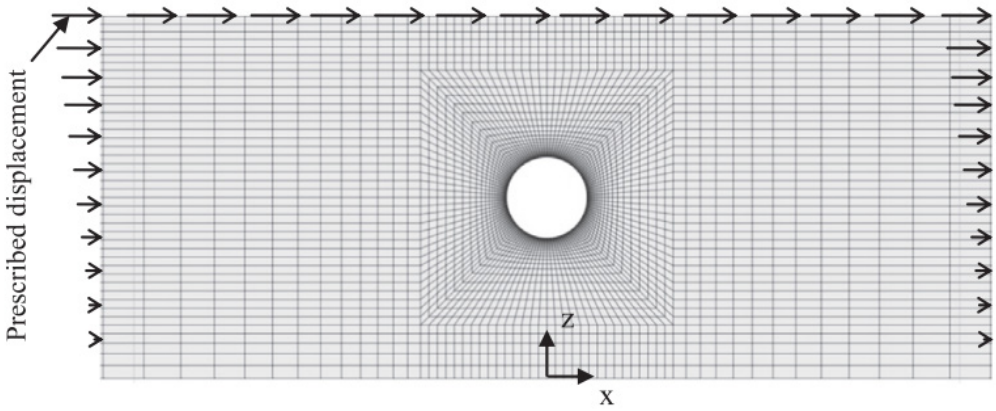

Figure 3. Geometry and quasi-static loading conditions for the circular tunnel model [25].

The mesh is composed of a single layer of zones in the y-direction, and the element's dimension increases as one moves away from the tunnel. It reaches the maximum size of 2.6 × 1 m at the model boundary (Figure 3). The boundary conditions of the numerical model are 120 m in the x-direction and 40 m in the z-direction. It consists of approximately

4800 zones and 9802 nodes. The bottom of the model was blocked in all directions, and the vertical sides were fixed in the horizontal one.

In this study, similar to the research work of Sederat et al. [15], Do et al. [25], and Naggar and Hinchberger [26], ovaling deformations due to the seismic loading are imposed as inverted triangular displacements, along with the model lateral boundaries. Uniform horizontal displacements are applied along the top boundary (Figure 3). The magnitude of the prescribed displacements assigned at the top of the model is dependent on the maximum shear strain γ_{max}, estimated based on the horizontal acceleration a_H. The bottom of the model is restrained in all directions.

Before applying the ovaling deformation due to seismic loading, a steady state of the excavated tunnel under static conditions was established. When the tunneling process is performed in a 2D plane strain model, it is assumed that ground displacements surrounding the tunnel boundary prior to the lining installation are simulated by using the convergence confinement method with a relaxation factor, λ_d, equal to 0.3 [25,27]. The numerical simulation of the tunnel ovaling was therefore performed through the following steps:

- Step 1: In situ state of stresses before tunnel construction.
- Step 2: Excavation of the tunnel and use of the convergence confinement process with a relaxation factor, γ_d, of 0.3. The concrete lining is then activated on the tunnel's periphery.
- Step 3: Assigning ovaling deformations caused by the seismic loading on the model boundaries using the prescribed displacements previously mentioned.

It should be noted that only incremental internal forces are presented in this study. They are determined by subtracting the total lining forces computed at the end of the static loading (step 2) from those determined at the end of the ovaling step (step 3).

2.3. Comparison of the Numerical and Analytical Model for the Circular Tunnel Case Study

For validation purposes of the numerical model subjected to quasi-static loading, the well-known analytical solution proposed by Wang [9], and thereafter improved by Kouretzis [16], was used for comparison with the results obtained from the numerical model. Several authors showed that this solution is efficient and can be used for the seismic design of circular tunnels [12,25]. It should be noted that Kouretzis [16] proposed an expression of the maximum incremental bending moment under the no-slip condition, which was not mentioned by Wang [9]. Parameters shown in Table 1 were adopted in this section as the reference case. The soil and tunnel lining material properties in numerical models were assumed to be linear elastic and massless. These assumptions were also adopted in the analytical solution. An anisotropic stress field was assigned in the numerical model with a lateral earth pressure coefficient at rest, K_0, of 0.5.

Figure 4 illustrates the distribution of the incremental internal forces induced in the tunnel lining under seismic loading. The conditions of lining and soil interaction, when using the Wang solution and FLAC^{3D}, were considered for both cases of no slip and full slip. The soil and tunnel lining parameters fed into the model are presented in Table 1. The results obtained by numerical and analytical models are in good agreement. Figure 4a,c show that the maximum incremental bending moment in the full-slip case is 14% larger than that obtained in the no-slip case. In contrast, the maximum incremental normal forces in the full-slip case are smaller than those in the no-slip case (Figure 4b,d).

Table 1. Input parameters for the reference case study.

Parameter	*Symbol*	*Unit*	*Value*
Soil properties			
Unit weight	γ	kN/m^3	18
Young's modulus	E	MPa	100
Poisson's ratio	ν	-	0.34
Internal friction angle	ϕ	degrees	33
Cohesion	c	kPa	0
Lateral earth pressure coefficient	K_0	-	0.5
Depth of tunnel	H	m	20
Peak horizontal acceleration at ground surface	a_H	g	0.5
Tunnel lining properties			
Young's modulus	E_l	GPa	35
Poisson's ratio	ν_l	-	0.15
Lining thickness	t	m	0.5
External diameter	D	m	9.76

In the section below, a parametric study is conducted to highlight the behavior of circular tunnel lining subjected to quasi-static loadings considering the effect of Young's modulus E, horizontal seismic acceleration a_H, and tunnel lining thickness t variations. Parameters of the soil and tunnel lining presented in Table 1 are adopted for the reference case study.

Both maximum and minimum incremental bending moments are presented. They are both labelled "extreme incremental bending moment". Similarly, extreme incremental normal forces representing both the maximum and minimum incremental normal forces induced in the tunnel lining are presented.

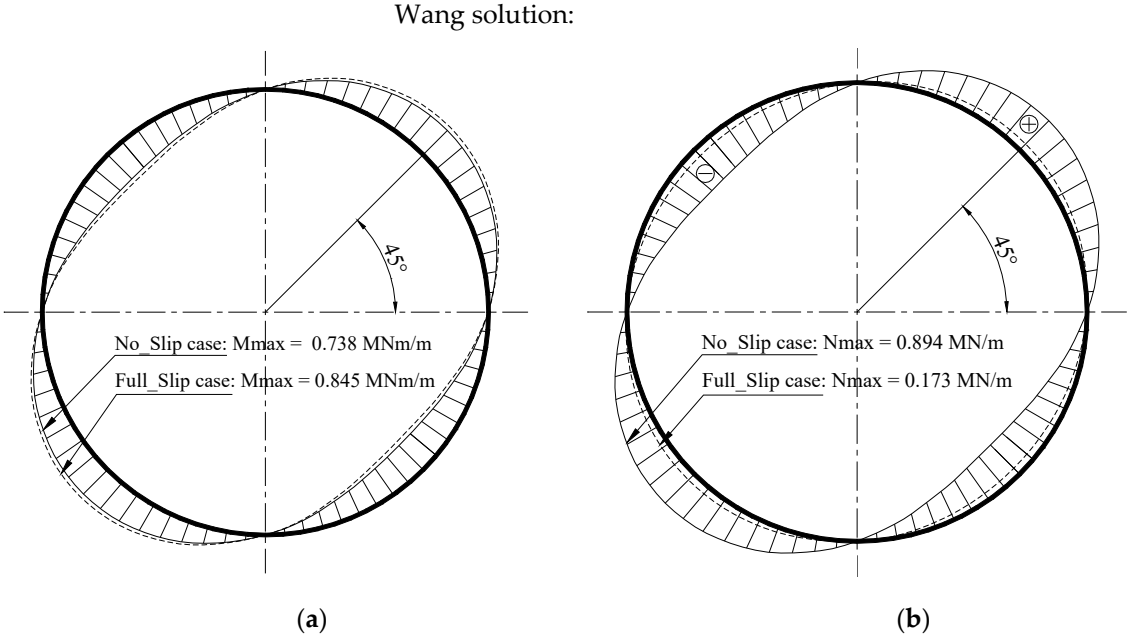

Figure 4. *Cont.*

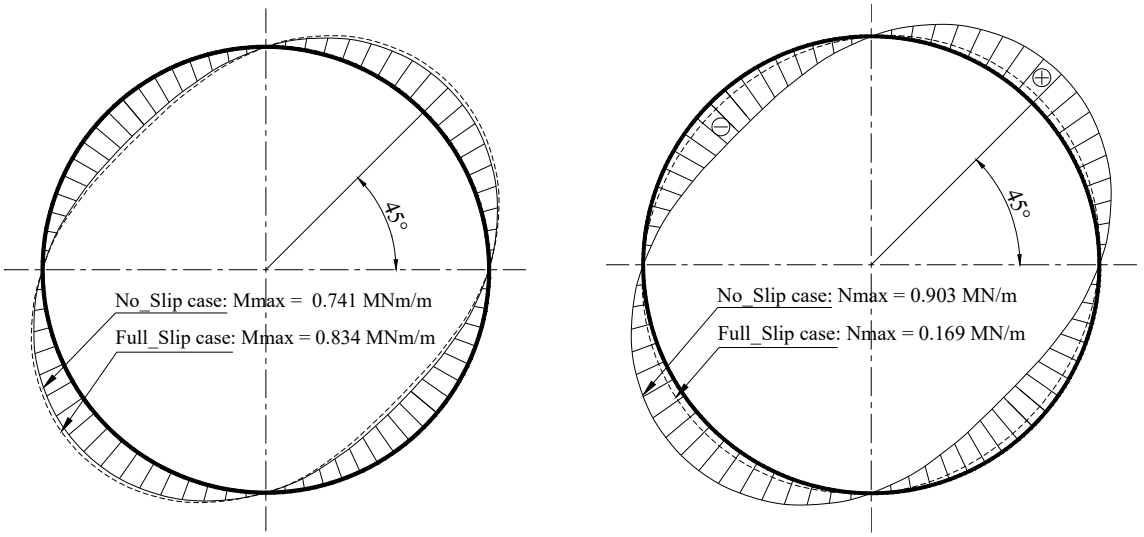

(**c**) (**d**)

Figure 4. Distribution of the incremental internal forces in the circular tunnel by FLAC^{3D} and Wang solution. (**a**) Incremental bending moments; (**b**) incremental normal forces; (**c**) incremental bending moments; (**d**) incremental normal forces.

2.3.1. Effect of the Peak Horizontal Seismic Acceleration (a_H)

A parametric study was conducted to investigate the seismic loading magnitude effects represented here by the maximum horizontal acceleration, a_H. The maximum horizontal acceleration is varied in the range between 0.05 and 0.75 g, corresponding to the respectively maximum shear strains, γ_{max}, of 0.038 and 0.58%. The other parameters of the reference case in Table 1 are used. The following conclusions can be deduced from Figure 5:

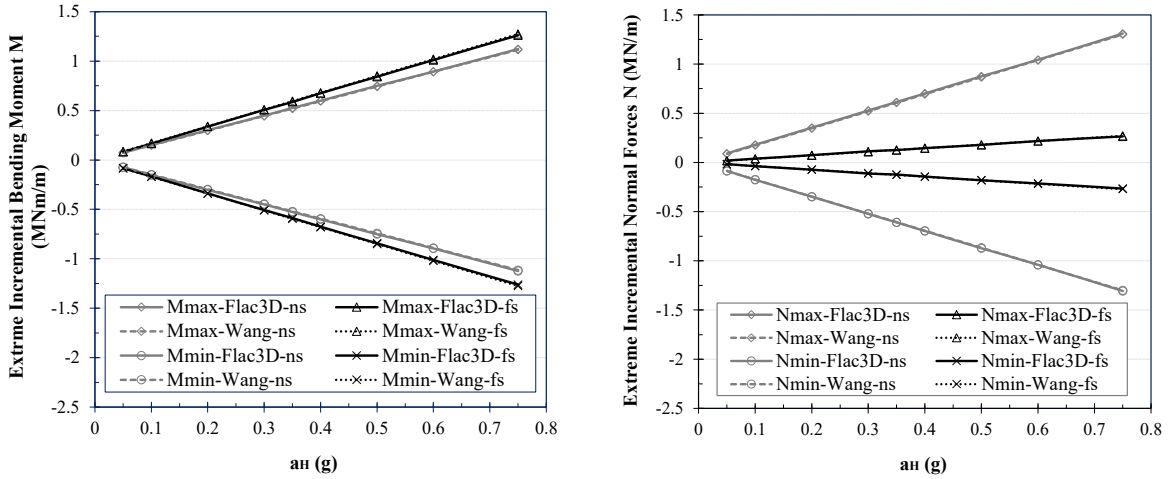

(**a**) (**b**)

Figure 5. Effect of a_H on the extreme incremental internal forces of the circular tunnel lining. (**a**) Extreme incremental bending moments; (**b**) Extreme incremental normal forces.

For both the no-slip and full-slip conditions, numerical results show good agreement with the analytical solution. A discrepancy of approximately 1% for both the extreme incremental bending moments and normal forces is obtained.

The absolute values of the extreme incremental bending moments and normal forces increased gradually with the a_H increase from 0.05 to 0.75 g. Incremental bending moments

for both no-slip and full-slip conditions are strongly dependent on the a_H value (Figure 5a). However, while incremental normal forces in the tunnel lining for the no-slip condition are strongly affected by the a_H value, insignificant incremental normal forces variations due to a_H for the full-slip condition are observed (Figure 5b).

2.3.2. Effect of the Soil Young's Modulus E

The soil Young's modulus is assumed to fall in a range from 10 to 350 MPa. The other parameters presented in Table 1, based on the reference case study, were used as the input data. The numerical results obtained by using the FLAC^{3D} comparison with Wang's analytical method for the full-slip and no-slip conditions are presented in Figure 6. The observations discussed below were made.

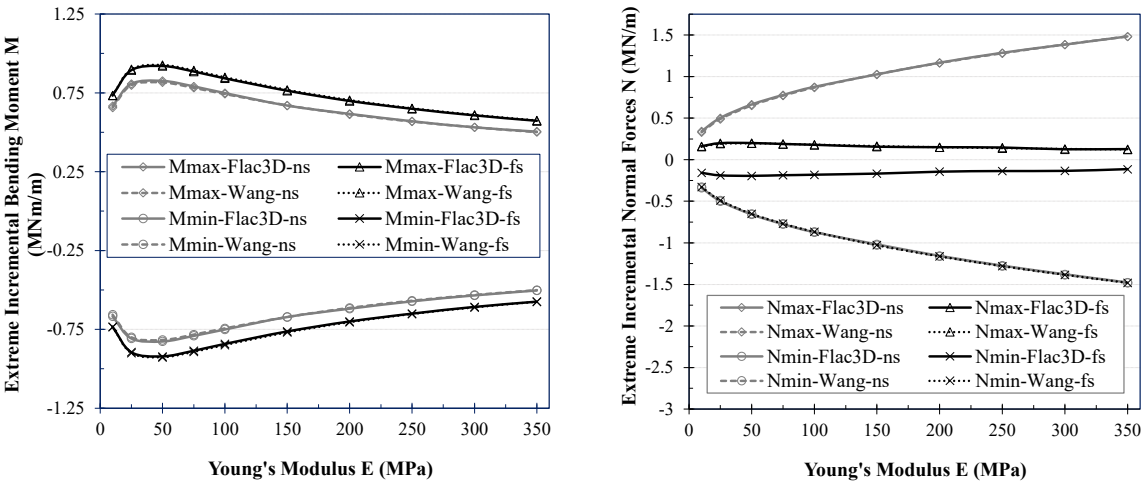

(**a**) (**b**)

Figure 6. Effect of E on the incremental internal forces of the circular tunnel lining. (**a**) Extreme incremental bending moments; (**b**) extreme incremental normal forces.

Figure 6 shows good agreement of the incremental bending moments and normal forces induced in the tunnel lining under seismic loading, obtained by the numerical model and the analytical solution for both no-slip and full-slip conditions when considering the E variation. The maximum difference is smaller than 2%.

The extreme incremental bending moments are strongly dependent on the E value as seen in Figure 6a. The absolute values of the extreme incremental bending moments are reached for E values close to 50 MPa. There is a rapid decrease in the absolute extreme incremental bending moments when the E value reduces from 25 to 10 MPa. When the E values are larger than 50 MPa, an increase in E induces a decrease in the absolute extreme incremental bending moments. This correlation of the extreme incremental bending moments is observed in both full-slip and no-slip conditions. It should be noted that for the same E value, the absolute extreme incremental bending moments induced in the tunnel lining for the no-slip condition are always 10 to 15% smaller than the full-slip ones.

While the extreme incremental normal forces in the full-slip conditions are insignificantly dependent on the E value (Figure 6b), an increase in E can cause a rapid increase in the maximum and minimum incremental normal forces in the tunnel lining for the no-slip condition. As predicted, incremental normal forces for the no-slip condition are always larger than the full-slip ones.

2.3.3. Effect of the Lining Thickness

The tunnel lining thickness was assumed to vary between 0.2 to 0.8 m, corresponding to a lining thickness vs. tunnel dimension ratio of 3 to 8.5% [28], while the other parameters are based on the reference case assumed in Table 1. Similar to what happens when

considering the soil Young's modulus E and horizontal seismic acceleration a_H effects, the results presented in Figure 7 show good agreement between analytical and numerical models for both no-slip and full-slip conditions. The discrepancy is under 1% for both the incremental bending moments and normal forces.

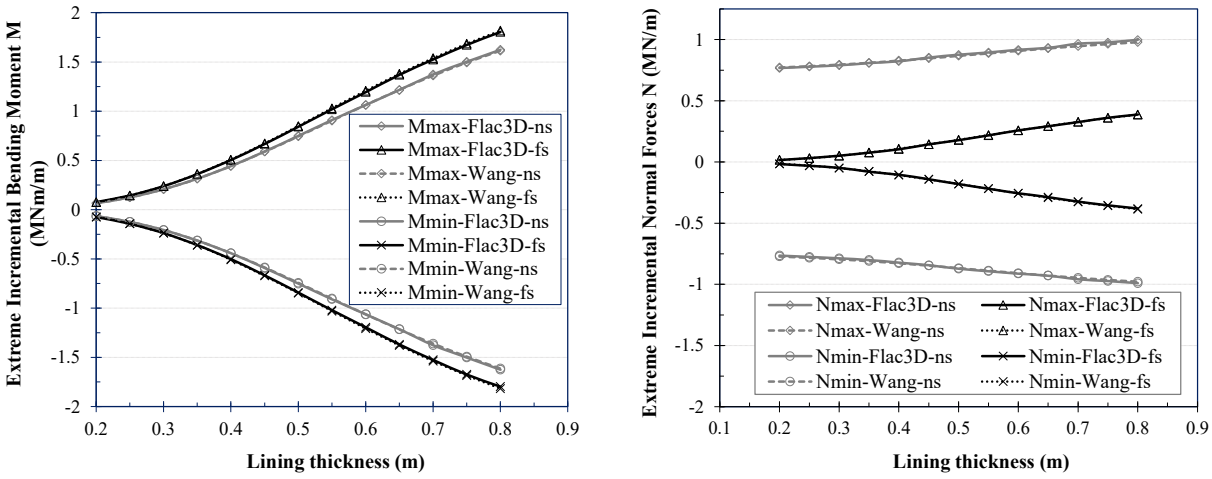

(**a**) (**b**)

Figure 7. Effect of the lining thickness on the incremental internal forces in the circular tunnel lining. (**a**) Extreme incremental bending moments; (**b**) extreme incremental normal forces.

In general, the absolute extreme incremental bending moment and normal force values gradually increase when the lining thickness t increases from 0.2 to 0.8 m. This concerns both the full-slip and no-slip conditions. The incremental bending moments for the no-slip condition are always smaller than the full-slip ones (Figure 7a). The biggest difference of 14% was obtained for a lining thickness of 0.8 m. It should be noted that the incremental normal forces variations caused by the lining thickness increase are less significant when compared to the incremental bending moment ones (Figure 7a,b).

Based on the above comparison between the analytical solution and numerical model when considering Young's modulus E, horizontal seismic acceleration a_H, and tunnel lining thickness t, which show good agreement between the analytical solution and numerical model, it is reasonable to conclude that the circular tunnel numerical model developed can be used to investigate the behavior of circular tunnels subjected to seismic loadings.

2.4. Development of a Numerical Model for Sub-Rectangular Tunnels

In this section, a numerical model was developed for the sub-rectangular tunnel case using similar soil parameters, lining material, and modeling processes to consider the static and seismic loadings introduced above. The tunnel shape is modified into a sub-rectangular geometry, and the gravity effect is taken into consideration. The mesh consists of a single layer of zones in the y-direction, and the dimension of the elements increases as one moves away from the tunnel (Figure 8). The geometry parameters of sub-rectangular tunnels are presented in Figure 1, and other parameters presented in Table 1 are adopted. The numerical model is 120 m wide in the x-direction, 40 m high in the z-direction, and consists of approximately 5816 elements and 11,870 nodes. The bottom of the model was blocked in all directions, and the vertical sides were fixed in the horizontal one.

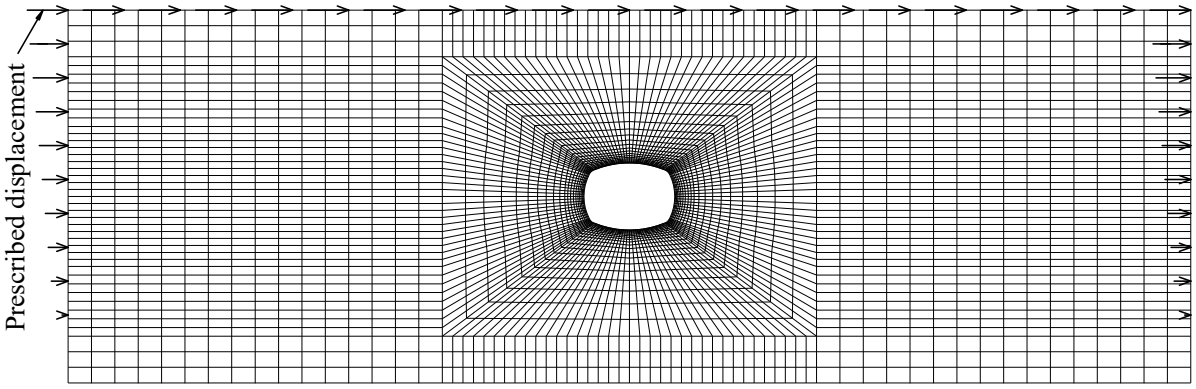

Figure 8. Geometry and quasi-static loading conditions in the numerical model of a sub-rectangular tunnel.

3. Parametric Study of Sub-Rectangular Tunnels in Quasi-Static Conditions

Figure 9 introduces the incremental bending moments and normal forces induced in the sub-rectangular tunnel linings subjected to seismic loadings and considers both no-slip and full-slip conditions. Parameters of the reference case presented in Table 1 are adopted.

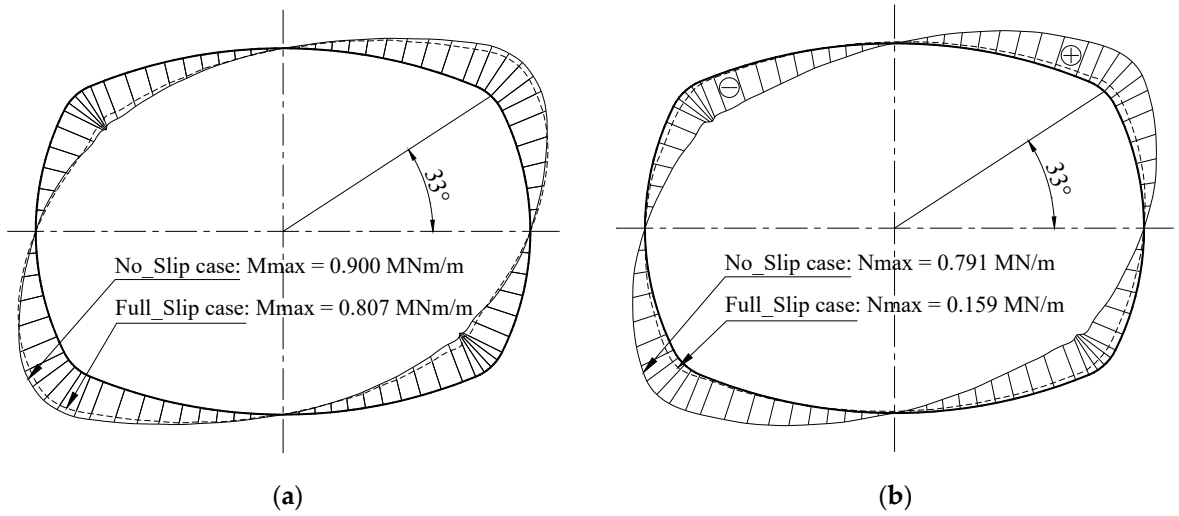

Figure 9. Distribution of the incremental bending moments and normal forces in the sub-rectangular tunnel. (**a**) incremental bending moment; (**b**) incremental normal forces.

Figures 4 and 9 provide a clear understanding of the behavior of circular and sub-rectangular tunnel linings under seismic loadings. The positions at the tunnel periphery, where the extreme incremental internal forces are reached, are positioned. It can be seen from Figure 9 that extreme incremental bending moments and normal forces observed in the sub-rectangular tunnel appear at the tunnel lining corners where the smaller lining radii are located. In the following sections, a numerical investigation was conducted to highlight the behavior of a sub-rectangular tunnel compared with a circular shape. These two tunnels have the same utilization space area and are twice subjected to seismic loadings while considering the effect of parameters, such as the horizontal seismic acceleration, soil deformation modulus, and lining thickness. The effects of the soil–lining interface condition are also investigated.

3.1. Effect of the Peak Horizontal Seismic Acceleration (a_H)

Shear strain values corresponding to a range of a maximum horizontal acceleration varying from 0.05 and 0.75 g were adopted in this study. In general, high seismic loadings are implied by a high horizontal acceleration a_H, and therefore shear strain values of γ_{max},

and result in high absolute extreme incremental bending moments and normal forces. The relationship is quite linear (Figure 10).

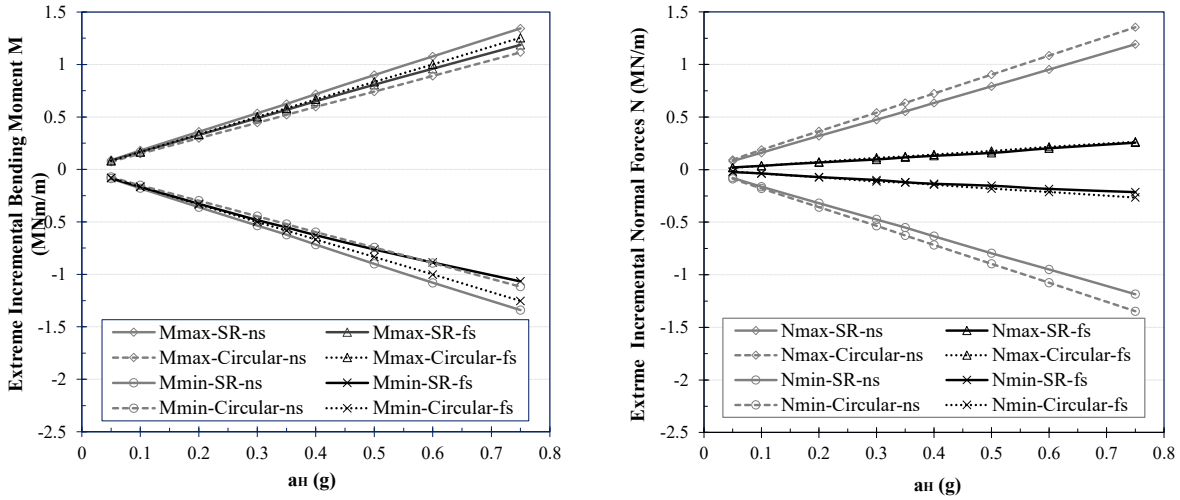

(**a**) (**b**)

Figure 10. Effect of the a_H value on the internal forces of circular and sub-rectangular tunnel linings. (**a**) Incremental bending moments; (**b**) incremental normal forces.

The results presented in Figure 10a show that, for the no-slip condition, absolute extreme incremental bending moments in the sub-rectangular lining are 20% larger than the circular ones. Nevertheless, for the full-slip condition, absolute extreme incremental bending moments in the circular lining are approximately 4% greater than the sub-rectangular ones. In the case of sub-rectangular linings, absolute extreme incremental bending moments for the full-slip condition are always lower by about 10% than the no-slip ones. This relationship is opposite to that observed in the cases of the circular-shaped tunnel (Figure 10a).

It can be seen in Figure 10b that for both shapes of tunnels, the absolute extreme incremental normal forces for the no-slip condition are approximately 80% larger than the full-slip ones. Unlike the incremental bending moments mentioned above, the absolute extreme incremental normal forces of the sub-rectangular lining are approximately 9% lower than the circular lining ones, for both the no-slip and full-slip conditions and when changing the horizontal acceleration (Figure 10b).

3.2. Effect of the Soil Young's Modulus (E)

The soil Young's modulus values are assumed to vary in the range from 10 to 350 MPa while keeping K_0 equal to 0.5 and a_H of 0.5 g. The other parameters based on the reference case are assumed (Table 1). The following can be seen from Figure 11.

For low E values smaller than 50 MPa, an increase in E induces an increase in the absolute extreme incremental bending moments. When the E value is greater than 50 MPa, the increase in E causes a decrease in the absolute extreme incremental bending moments (Figure 11a). It should be noted that the dependency of the absolute extreme incremental bending moments in the sub-rectangular tunnels on the E value is insignificant compared to the circular-shaped tunnels (Figure 11a). It is also worth highlighting that while the absolute extreme incremental bending moments of the circular tunnel for the no-slip condition are smaller than the corresponding full-slip ones [9,25], the absolute extreme incremental bending moments of the sub-rectangular tunnel for the no-slip condition are greater than the corresponding full-slip ones. The behavior of sub-rectangular tunnels is different from the circular-shaped tunnels. The same conclusion was also obtained when considering the horizontal seismic acceleration a_H.

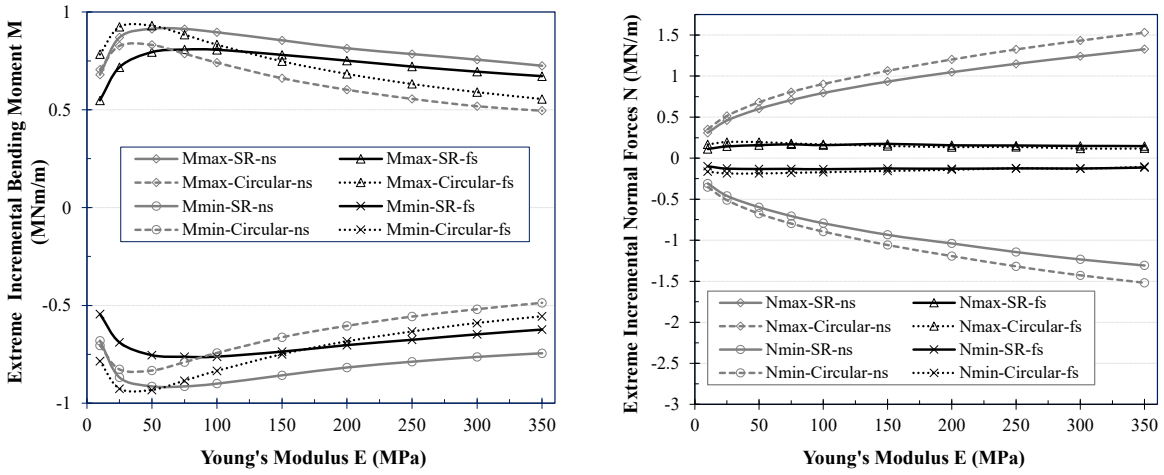

(**a**) (**b**)

Figure 11. Effect of the *E* value on the internal forces for the circular and sub-rectangular tunnel linings. (**a**) Incremental bending moments; (**b**) incremental normal forces.

Figure 11a also shows greater absolute extreme incremental bending moments induced in sub-rectangular tunnels for the no-slip condition compared with circular tunnels with the same utilization space area. However, in the full-slip condition, absolute extreme incremental bending moments in the circular tunnel are greater than the sub-rectangular ones for *E* values smaller than approximately 150 MPa. When *E* values are larger than 150 MPa, absolute extreme incremental bending moments developed in circular tunnels are smaller than in sub-rectangular tunnels.

Figure 11b indicates that an increase in *E* value causes a significant corresponding increase in the absolute extreme normal forces in both sub-rectangular and circular tunnels for the no-slip condition. However, it induces an insignificant change in absolute extreme incremental normal forces for the full-slip condition. Absolute extreme incremental normal forces in the sub-rectangular tunnels are generally 10% smaller than for the circular tunnels.

3.3. Effect of the Lining Thickness (t)

The lining thickness *t* is assumed to vary in the range between 0.2 and 0.8 m while keeping K_0 value of 0.5, an a_H value of 0.5 g, and an *E* value of 100 MPa. Other parameters introduced in Table 1 were adopted. The results presented in Figure 12 indicate that the lining thickness has a great effect on the incremental internal forces for both sub-rectangular and circular tunnels and in both no-slip and full-slip conditions. The relationship between the lining thickness and the incremental internal forces for the considered cases is quite linear.

For the no-slip condition, absolute extreme incremental bending moments of the sub-rectangular linings are always larger than the circular ones (Figure 12a). The discrepancy declined gradually from 124 to 6%, corresponding to the lining thickness increase from 0.2 to 0.8 m. In the full-slip conditions, considering a lining thickness smaller than approximately 0.5 m, the absolute extreme incremental bending moments of the sub-rectangular linings are still larger than the circular ones, similar to the no-slip condition presented earlier. However, when the lining thickness is larger than 0.5 m, the opposite result is obtained, as shown in Figure 12a. Thus, larger absolute extreme incremental bending moments on the circular tunnels are observed.

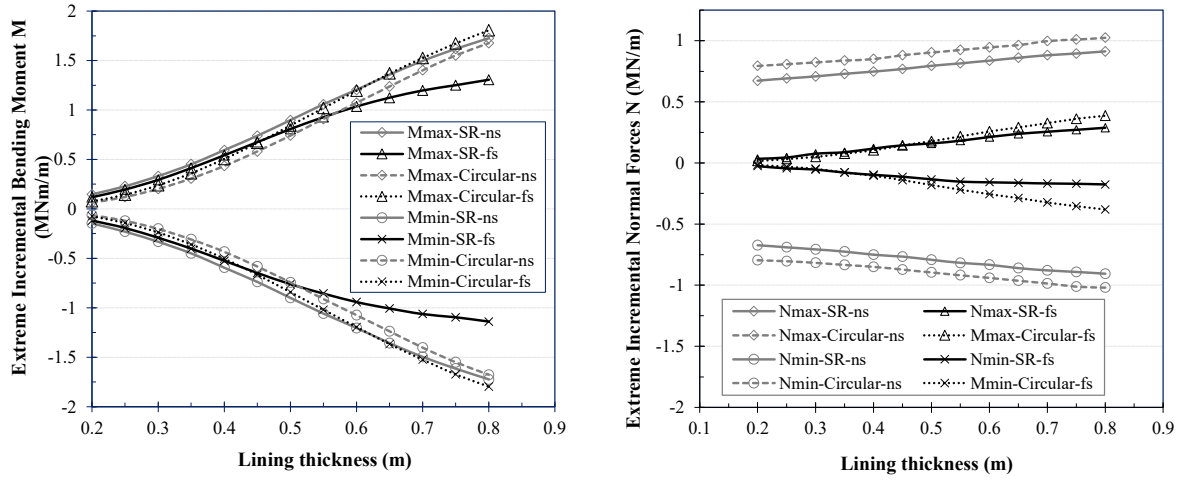

(**a**) (**b**)

Figure 12. Effect of the lining thickness on the incremental internal forces of the circular and sub-rectangular tunnel linings. (**a**) Incremental bending moments; (**b**) incremental normal forces.

It can be seen in Figure 12b that the incremental normal forces in the no-slip condition are always larger than the full-slip ones. In comparison with the incremental normal forces of the circular lining, the incremental normal forces in the sub-rectangular lining are lower by about 9 and 25% for no-slip and full-slip conditions, respectively (Figure 12b).

4. Conclusions

A 2D numerical study allowed an investigation of the behavior of sub-rectangular tunnel linings under seismic loadings. The influences of parameters, such as soil deformation, maximum horizontal acceleration, lining thickness, and soil–lining interface conditions, on the circular- and sub-rectangular-shaped tunnel behavior under seismic loading were investigated. Considerable differences in the response of these tunnels were observed. Based on the research results, the following conclusions can be drawn:

The horizontal acceleration a_H, the soil Young's modulus E, and lining thickness t have a great effect on the incremental internal forces induced in both sub-rectangular and circular tunnels for both no-slip and full-slip conditions.

In general, a higher seismic loading induced by a higher horizontal acceleration a_H will induce higher incremental bending moments and normal forces in both circular and sub-rectangular tunnels. The relationship is quite linear.

The results proved that soil–lining interface conditions have a great influence on the behavior of sub-rectangular tunnels. This is completely different when comparing the behavior of circular-shaped tunnels. Indeed, while the absolute extreme incremental bending moments of a circular tunnel for the no-slip condition are smaller than the corresponding full-slip ones, the absolute extreme incremental bending moments of sub-rectangular tunnels for the no-slip condition are greater than the corresponding full-slip ones. This represents an opposite trend to what can be observed in circular tunnel linings.

For all investigated case studies, absolute incremental normal forces for the no-slip conditions are always larger than the full-slip ones, for both the circular and sub-rectangular tunnels cases. Absolute extreme incremental normal forces in sub-rectangular tunnels are approximately 10% smaller than the circular ones.

The dependency of the absolute extreme incremental bending moments induced on the sub-rectangular tunnels on the soil Young's modulus (E) is insignificant compared with that on the circular ones. The soil Young's modulus of 50 MPa could be considered as a critical value for both tunnel shape cases. Beyond this value, the E increase induces a decrease in the absolute extreme incremental bending moments. However, below this

value, an increase in E value induces an increase in the absolute extreme incremental bending moments.

An increase in the soil Young's modulus (E) causes a significant corresponding increase in the absolute extreme incremental normal forces for both sub-rectangular and circular tunnels (no-slip condition). An insignificant change in the absolute extreme incremental normal forces is observed for the full-slip conditions.

The numerical results obtained in the present study are useful for the preliminary design of circular- and sub-rectangular-shaped tunnel linings under seismic loadings. The joint distribution influence in the segmental lining on the tunnel behavior will be considered in future research.

Author Contributions: V.V.P.: Methodology, software and validation, investigation, data curation, writing—original draft preparation. N.A.D.: Conceptualization, methodology, software and validation, writing—review and editing. D.D.: Conceptualization, methodology, writing—review and editing, supervision. All authors have read and agreed to the published version of the manuscript.

Funding: This research is supported by the Vietnam Ministry of Education and Training.

Institutional Review Board Statement: Not applicable.

Informed Consent Statement: Not applicable.

Conflicts of Interest: The authors declare no conflict of interest.

References

1. Skrzypkowski, K. Evaluation of Rock Bolt Support for Polish Hard Rock Mines. *E3S Web Conf.* **2018**, *35*, 01006. [CrossRef]
2. Cai, H.; Lu, A.Z.; Ma, Y.C.; Yin, C.L. Semi-analytical solution for stress and displacement of lined circular tunnel at shallow depths. *Appl. Math. Model.* **2021**, *100*, 263–281. [CrossRef]
3. Lu, A.Z.; Zeng, X.T.; Xu, Z. Solution for a circular cavity in an elastic half plane under gravity and arbitrary lateral stress. *Int. J. Rock. Mech. Min.* **2016**, *89*, 34–42. [CrossRef]
4. Lu, A.Z.; Cai, H.; Wang, S.J. A new analytical approach for a shallow circular hydraulic tunnel. *Meccanica* **2019**, *54*, 223–238. [CrossRef]
5. Nakamura, H.; Kubota, T.; Furukawa, M.; Nakao, T. Unified construction of running track tunnel and crossover tunnel for subway by rectangular shape double track cross-section shield machine. *Tunn. Undergr. Space Technol.* **2003**, *18*, 253–262. [CrossRef]
6. Zhang, Z.X.; Zhu, Y.T.; Zhu, Y.F.; Huang, X.; Zhuang, Q.W. Development and application of a 1:1 mechanical test system for special-shaped shield lining with a large cross-section. *Chin. J. Rock Mech. Eng.* **2017**, *12*, 2895–2905. (In Chinese)
7. Liu, X.; Ye, Y.; Liu, Z.; Huang, D. Mechanical behavior of Quasi-rectangular segmental tunnel linings: First results from full-scale ring tests. *Tunn. Undergr. Space Technol.* **2018**, *71*, 440–454. [CrossRef]
8. Jianbin, L. Key Technologies and Applications of the Design and Manufacturing of Non-Circular TBMs. *Engineering* **2017**, *3*, 905–914. [CrossRef]
9. Wang, J.N. *Seismic Design of Tunnels: A State-of-the-Art Approach*; Brinckerhoff Quade and Douglas Inc.: New York, NY, USA, 1993.
10. Penzien, Z. Seismically induced racking of tunnel linings. *Int. J. Earthq. Eng. Struct. Dynamic.* **2000**, *29*, 683–691. [CrossRef]
11. Bobet, A. Effect of pore water pressure on tunnel support during static and seismic. *Tunn. Undergr. Space Technol.* **2003**, *18*, 377–393. [CrossRef]
12. Hashash, Y.M.A.; Park, D.; Yao, J.I.C. Ovaling deformations of circular tunnels under seismic loading, an update on seismic design and analysis of underground structures. *Tunn. Undergr. Space Technol.* **2005**, *20*, 435–441. [CrossRef]
13. Naggar, H.E.; Hinchberge, S.D.; Hesham, M.; Naggar, E.I. Simplified analysis of sesmic in-plane stresses in composite and jointed tunnel linings. *Tunn. Undergr. Space Technol.* **2008**, *28*, 1063–1077.
14. Park, K.H.; Tantayopin, K.; Tontavanich, B.; Owatsiriwong, A. Analytical solution for seismic-induced ovaling of circular tunnel lining under no-slip interface conditions: A revisit. *Tunn. Undergr. Space Technol.* **2009**, *24*, 231–235. [CrossRef]
15. Sederat, H.; Kozak, A.; Hashash, Y.M.A.; Shamsabadi, A.; Krimotat, A. Contact interface in seismic analysis of circular tunnels. *Tunn. Undergr. Space Technol.* **2009**, *24*, 482–490. [CrossRef]
16. Kouretzis, G.; Sloan, S.W.; Carter, J.P. Effect of interface friction on tunnel liner internal forces due to seismic S- and P-wave propagation. *Soil Dyn. Earthq. Eng.* **2013**, *46*, 41–51. [CrossRef]
17. Nguyen, D.D.; Park, D.; Shamsher, S.; Nguyen, V.Q.; Lee, T.H. Seismic vulnerability assessment of rectangular cut-and-cover subway tunnels. *Tunn. Undergr. Space Technol.* **2019**, *86*, 247–261. [CrossRef]
18. Sun, Q.Q.; Du, D.; Dias, D. An improved Hyperstatic Reaction Method for tunnels under seismic loading. *Tunn. Undergr. Space Technol.* **2021**, *108*, 103687. [CrossRef]

19. Tsinidis, G.; Silva, F.D.; Anastasopoulos, I.; Bilotta, E.; Bobet, A.; Hashash, Y.M.; He, C.; Kampas, G.; Knappett, J.; Madabhushi, G.; et al. Seismic behaviour of tunnels: From experiments to analysis. *Tunn. Undergr. Space Technol.* **2020**, *99*, 103334. [CrossRef]
20. Kashima, Y.; Kondo, N.; Inoue, M. Development and application of the DPLEX shield method: Results of experiments using shield and segment models and application of the method in tunnel construction. *Tunn. Undergr. Space Technol.* **1996**, *11*, 45–50. [CrossRef]
21. Zhang, Z.; Zhu, Y.; Huang, X.; Zhu, Y.; Liu, W. "Standing" full-scale loading tests on the mechanical behavior of a special-shape shield lining under shallowly-buried conditions. *Tunn. Undergr. Space Technol.* **2019**, *86*, 34–50. [CrossRef]
22. Do, N.A.; Dias, D.; Zixin, Z.; Xin, H.; Nguyen, T.T.; Pham, V.V.; Ouahcène, N.R. Study on the behavior of squared and sub-rectangular tunnels using the Hyperstatic Reaction Method. *Transp. Geotech.* **2020**, *22*, 100321. [CrossRef]
23. Nguyen, T.T.; Do, N.A.; Karasev, M.A.; Dang, V.K.; Dias, D. Influence of Tunnel Shape on Tunnel Lining Behavior. *Proc. ICE—Geotech. Neuroeng.* **2020**, *174*, 355–371. [CrossRef]
24. Itasca Consulting Group. FLAC Fast Lagrangian Analysis of Continua, Version 5.0. *User's Manual*. Available online: https://www.itascacg.com/ (accessed on 10 April 2021).
25. Do, N.A.; Dias, D.; Oreste, P.P.; Djeran-Maigre, I. 2D Numerical Investigation of Segmental Tunnel Lining under Seismic Loading. *Soil Dyn. Earthq. Eng.* **2015**, *72*, 66–76. [CrossRef]
26. Naggar, H.E.; Hinchberger, S.D. Approximate evaluation of stresses in degraded tunnel linings. *Soil Dyn. Earthq. Eng.* **2012**, *43*, 45–57. [CrossRef]
27. Möller, S.C.; Vermeer, P.A. On numerical simulation of tunnel installation. *Tunn. Undergr. Space Technol.* **2008**, *23*, 461–475. [CrossRef]
28. FHWA-HIF-20-035. *Precast Concrete Segmental Liners for Large Diameter Road Tunnels-Literature Survey and Synthesis*; WSP USA, Inc.: Baltimore, MD, USA, 3 October 2020. Available online: https://www.fhwa.dot.gov/bridge/tunnel/pubs/hif20035.pdf (accessed on 3 October 2021).